

## Article

# Mercury Enrichment Characteristics and Rhizosphere Bacterial Community of Ramie (*Boehmeria Nivea* L. Gaud.) in Mercury-Contaminated Soil

Xiuhua Li <sup>1,2</sup>, Xiaomi Wang <sup>1</sup>, Ling Zhao <sup>1</sup>, Zuopeng Wang <sup>1,2</sup>, Ying Teng <sup>1,\*</sup> and Yongming Luo <sup>1</sup>

<sup>1</sup> CAS Key Laboratory of Soil Environment and Pollution Remediation, Institute of Soil Science, Chinese Academy of Sciences, Nanjing 210008, China; xhli@issas.ac.cn (X.L.); xmwang@issas.ac.cn (X.W.); zhaoling@issas.ac.cn (L.Z.); wangzuopeng@issas.ac.cn (Z.W.); ymluo@issas.ac.cn (Y.L.)  
<sup>2</sup> University of the Chinese Academy of Sciences, Beijing 100049, China  
\* Correspondence: yteng@issas.ac.cn; Tel.: +86-025-86881531

**Abstract:** Phytoremediation is a promising technique for reducing mercury (Hg) pollution. Little is known about the phytoremediation potential of ramie (*Boehmeria nivea* L. Gaud.) and the response of its rhizosphere soil microbiome to Hg contamination. In this study, we planted ramie in three plots contaminated with different levels of Hg pollution and evaluated ramie Hg accumulation and translocation. We also analyzed the abundance, composition, and predominant taxa of the rhizosphere soil bacterial community. Results showed that the average THg concentration decreased by 30.80%, 18.36%, and 16.31% in plots L, M, and H, respectively. Ramie displayed strong Hg tolerance and good Hg accumulation performance, especially in soil contaminated with a low level of Hg. After ramie planting, soil SOM and CEC increased while pH, Eh, and THg content decreased in rhizosphere soil. Proteobacteria, Actinobacteriota, Gemmatimonadota, Latescibacterota, and NB1-j were identified as potential Hg-tolerant taxa at the phylum level, and their abundance increased in highly Hg-contaminated soil. Redundancy and correlation analyses indicated that soil bacterial community structure was significantly correlated with soil pH, Eh, and Hg content. This study provides a better understanding of the phytoremediation capacity of ramie and its rhizosphere function and thus lays a theoretical foundation for the phytoremediation of Hg-contaminated soils.



**Citation:** Li, X.; Wang, X.; Zhao, L.; Wang, Z.; Teng, Y.; Luo, Y. Mercury Enrichment Characteristics and Rhizosphere Bacterial Community of Ramie (*Boehmeria Nivea* L. Gaud.) in Mercury-Contaminated Soil. *Sustainability* **2023**, *15*, 6009. <https://doi.org/10.3390/su15076009>

Academic Editor: Zhihua Xiao

Received: 28 February 2023

Revised: 16 March 2023

Accepted: 29 March 2023

Published: 30 March 2023



**Copyright:** © 2023 by the authors. Licensee MDPI, Basel, Switzerland. This article is an open access article distributed under the terms and conditions of the Creative Commons Attribution (CC BY) license (<https://creativecommons.org/licenses/by/4.0/>).

**Keywords:** mercury; phytoremediation; *Boehmeria nivea* L.; soil; bacteria

## 1. Introduction

The heavy metal (HM) mercury (Hg) is a highly neurotoxic, globally distributed pollutant that enters the environment through both natural processes and anthropogenic activities [1,2]. The Wanshan Mercury Mine District is the largest former-Hg-producing district in Guizhou Province, China. Long-term mining and smelting activities resulted in serious soil Hg pollution at this site and associated socioeconomic and ecological problems [3].

Phytoremediation is one of the most cost-effective and eco-friendly technologies for remediating HM-polluted soil [4]. Efficient phytoremediation relies on the judicious selection of plant species [5]. For phytoremediation, the two most important plant characteristics are 1) high biomass production and 2) uptake of large quantities of HMs in aboveground tissues [6]. Ramie (*Boehmeria nivea* L. Gaud.), a perennial herbaceous plant with a long history of cultivation around the world, is widely used for phytoremediation. Ramie is characterized by extensive adaptability, fast growth, large biomass production, and dense rooting; moreover, ramie has strong resistance to various HMs and high HM-enrichment capacity [7]. Ramie grows well under high concentrations of Cd, Pb, and As [8]; can effectively absorb and translocate HMs to aboveground plant parts; and primarily accumulates HMs

in its roots [9]. However, there have been few studies of the phytoremediation potential of ramie in Hg-contaminated soil [10].

Plant roots not only accumulate HMs from the surrounding soil but also release root exudates into the rhizosphere soil. These root exudates can sustain a rich rhizosphere microbial community [11]. The rhizosphere environment is a very important soil–microbiome interface for element cycles and energy exchange [12]. The composition of the rhizosphere microbial community is affected by many factors, including soil physicochemical properties, plant species, and HM content [13]. Introducing plants can change soil pH and organic compound content, and these changes can promote the abundance and diversity of the soil microbial community [14]. Moreover, the root exudates of plants and, consequently, the rhizosphere environment vary [15]. The addition of Hg may alter the soil microbial community by influencing the relative abundance of major species [16]. Rhizosphere microorganisms also play an important role in managing soil ecosystems [17]. They regulate element and geochemical cycles, reduce the toxicity of HMs to plants, and increase plant HM accumulation and translocation [18]. Furthermore, some rhizosphere bacteria can transform HM fractions and contribute to phytoremediation processes [19,20]. These critical functions underscore the necessity of studying changes in the rhizosphere microbial community in Hg-contaminated soils.

In this study, an in situ phytoremediation experiment was carried out on farmland near the Wanshan Mercury Mine District. The soils in this area have been exposed to Hg contamination for more than 40 years, and there has been sufficient time for soil microorganisms to adapt to Hg contamination with different levels. Ramie was planted in three plots with different concentrations of Hg in the soil. The objectives of this study were to: (1) determine the accumulation and translocation characteristics of Hg in ramie; (2) analyze rhizosphere soil ecological characteristics (such as bacterial community structure and composition); and (3) explore the influence of Hg contamination and environmental variables on soil bacterial community structures. The findings in our study might be able to provide further understanding of the interactions between plants and microbes that are sustainable for soil remediation.

## 2. Materials and Methods

### 2.1. Site Description

The field experiment was conducted on farmland in Tongren City, Guizhou Province, southwestern China (109°15′05″ E, 27°27′33.72″ N). The study site is a typical karstic terrain mountain area rich in Hg ore, which is known as the “Hg capital” of China. It has a subtropical humid monsoon climate with a mean annual temperature of 17 °C, and a mean annual precipitation of 1250 mm. The long history of Hg mining and smelting has led to serious soil Hg contamination in the area. The soil properties and Hg contamination levels in this region are highly heterogeneous. The soil pH ranges from 4.89 to 8.38, the soil organic matter content ranges from 31.2 to 57.5 g·kg<sup>-1</sup>, and the soil Hg content ranges from 0.07 to 128 mg·kg<sup>-1</sup> [21].

### 2.2. Experimental Design

We selected three plots with different levels of Hg pollution: low (L), 10.50 ± 1.50 mg·kg<sup>-1</sup>; medium (M), 44.40 ± 1.48 mg·kg<sup>-1</sup>; and high (H), 88.07 ± 11.17 mg·kg<sup>-1</sup>. Each plot was approximately 20 m × 20 m (400 m<sup>2</sup>) and surrounded by a 0.25 m-wide ditch for drainage. Ramie seedlings (Xiangsi No.1, Research Institute of Hunan Agricultural University Changsha, China) in 40 cm × 40 cm (length × width) pots were transplanted into the three plots in April 2019 and grown for 6 months.

### 2.3. Sample Collection

In each plot, three quadrats (4 m × 4 m) containing ramie plants of similar growth and height were identified. Five ramie samples were collected from the 16-m<sup>2</sup> area surrounding the center sampling point and mixed together to form a single composite sample. The com-

posite sample was separated into four fractions: roots, leaves, stems, and bast (epidermis stripped from the stem). After collection, all plant samples were washed with deionized water thoroughly, freeze-dried, ground to a fine powder, and stored until further analysis.

A composite bulk soil sample (0–20 cm depth) of approximately 1.0 kg was also collected from each quadrat. In addition, the rhizosphere soil was collected from the root zone of each ramie sample by gently brushing with a sterile spatula. Each rhizosphere soil sample was divided into two subsamples with different usage: one was for chemical analysis and the other was for bacterial analysis. The soil samples for chemical analysis were first freeze-dried and then sieved through a 2 mm mesh. The subsamples for bacterial analysis were immediately stored at  $-80\text{ }^{\circ}\text{C}$  and used for DNA extraction.

#### 2.4. Chemical Analyses

Soil pH was determined with a glass electrode linked to a pH meter at a soil–distilled water ratio of 1:2.5 (*w/v*). Soil organic matter (SOM) was determined using the  $\text{K}_2\text{CrO}_7$  oxidation titration method. Soil Eh (redox potential) was measured at a soil–distilled water ratio of 1:2.5 (*w/v*) with an Eh meter. Soil CEC (cation exchange capacity) was measured by displacing exchangeable cations on soil particles with  $\text{NH}_4^+$  and determining  $\text{NH}_4^+$  [22].

Total Hg (THg) in soil and plants was determined following the method of Zhu et al. [23]. Soil samples ( $\sim 0.20\text{ g}$ ) were digested in 5 mL of aqua regia (3:1 HCl:  $\text{HNO}_3$ , *v/v*) with a water bath at  $100\text{ }^{\circ}\text{C}$  for 2 h. Following this, the digestion was diluted to 25 mL with ultrapure water. Root or aerial part samples ( $\sim 0.20\text{ g}$ ) were mixed with  $\text{HNO}_3$  (5 mL) and  $\text{H}_2\text{O}_2$  (3 mL) in a digestion vessel, heated at  $140\text{ }^{\circ}\text{C}$  for 4 h, and then the digestion was diluted to 25 mL with ultrapure water. The Hg concentration in the digestion was determined with atomic fluorescence spectrophotometry (Model AFS-930 Jitian, Beijing, China). Fluorescence is sensitive to Hg, and the detection limit was lower than  $0.001\text{ }\mu\text{g L}^{-1}$ .

Five chemical fractions were extracted sequentially according to the Tessier sequential extraction procedure [24]: F1: exchangeable fraction, F2: carbonate-binding fraction, F3: Fe–Mn oxide-binding fraction, F4: organic matter-binding fraction, and F5: residual fraction. The Hg concentration in each digestion was determined with atomic fluorescence spectrophotometry (Model AFS-930 Jitian, Beijing, China).

#### 2.5. Extraction, Sequencing, and Processing of Soil Bacterial DNA

Bacterial DNA was extracted from the soil samples ( $\sim 0.5\text{ g}$ ) using a soil genomic DNA kit (GeneMark, GMBiolab Co., Ltd., Taichung, Taiwan) following the manufacturer's instructions. The DNA concentration and purity were determined with a NanoDrop 2000 UV–vis spectrophotometer. The variable V4–V5 region of the bacterial 16S rRNA gene was amplified by PCR with the primers 515 F (5'-GTGCCAGCMGCCGCGG-3') and 907 R (5'-CCGTCAATTCCTTTGAG-3'). The PCR program was operated as follows: first, initial denaturation took place at  $95\text{ }^{\circ}\text{C}$  for 2 min followed by 25 cycles of denaturation at  $95\text{ }^{\circ}\text{C}$  for 30 s and annealing at  $55\text{ }^{\circ}\text{C}$  for 30 s. Following this, elongation occurred at  $72\text{ }^{\circ}\text{C}$  for 30 s before an extension took place at  $72\text{ }^{\circ}\text{C}$  for 5 min. Sequencing was conducted using Novogene Technology Co., Ltd. (Beijing, China). The low-quality sequences were removed, and effective sequences were distinguished after sequencing. The sequence reads were quality filtered for further analysis [25].

#### 2.6. Statistical Analysis

After normalization of the sample sequence, operational taxonomic unit (OTU) clustering analysis and species classification analysis were conducted. A cloud platform developed by Novogene Technology Co., Ltd. (Beijing, China) was used for the sequence analysis. Shifts in soil bacterial diversity among different plots were evaluated via  $\alpha$ -diversity and  $\beta$ -diversity of the bacterial community.  $\alpha$ -diversity indexes were used to evaluate the diversity of the bacterial community, including Chao 1, ACE, Shannon and Simpson index.  $\beta$ -diversity analysis was used to evaluate the similarities and differences in different treatments, and the principal coordinate analysis (PCoA) was used to analyze  $\beta$ -diversity in

this study. The differences between multiple sets of data on a two-dimensional coordinate graph were visualized to use variance decomposition [14]. The linear discriminant analysis effect size (LEfSe) method was used to identify the biomarkers that are associated with significant differences in the bacterial community and biological properties for a range of classes in different plots [11]. Redundancy analysis (RDA) was performed to characterize the effects of environmental variables on the bacterial communities in the three plots. Spearman correlation analysis was used to analyze the relationships between soil environmental factors and the ten most abundant phyla.

Differences were tested for significance via analysis of variance (ANOVA). Subsequent multiple comparisons among means were examined according to the least significance difference (LSD) and Duncan test ( $p < 0.05$ ) in SPSS 20.0. All graphics were generated using Origin 8.0.

### 3. Results and Discussion

#### 3.1. Total Mercury Concentration in Soil and Plants

To investigate the phytoremediation potential of ramie in Hg-contaminated soils, the soil concentration of THg was determined before and after ramie planting. As shown in Figure 1, ramie planting significantly reduced the soil THg concentrations in plots L and M ( $p < 0.05$ ). The average THg concentration decreased by 30.80%, 18.36%, and 16.31% in plots L, M, and H, respectively. THg is commonly determined by atomic fluorescence spectrophotometry (AFS) and inductively coupled plasma mass spectrometry (ICP-MS). ICP-MS is often used to determine Hg isotopes coupled with a direct mercury analyzer (DMA) [26]. AFS is frequently used for Hg determination since Hg is sensitive to fluorescence with detection limits lower than  $0.001 \mu\text{g L}^{-1}$ . Our results showed that Hg in soil could be determined through AFS. The decrease of Hg in different plot soils indicated that ramie was able to tolerate and accumulate Hg under diverse contamination conditions and confirmed that ramie was a promising plant species for the phytoremediation of HM-contaminated soil [5]. Qiao et al. considered that the Cd accumulated by *Brassica napus* L. roots was not all Cd in the rhizosphere soil but included the Cd in the bulk soil because of the migration of Cd in the soil. Though Cd could migrate in soil, the reduced rhizosphere Cd absorbed by roots could not be replenished by Cd in the bulk soil in time. The retardation could be mitigated by some acids [27]. Acidic root exudates could promote the migration of Cd from bulk soil to the rhizosphere soil. Therefore, the decrease of THg in bulk soil was caused by the migration of Hg from the bulk soil to the rhizosphere soil.

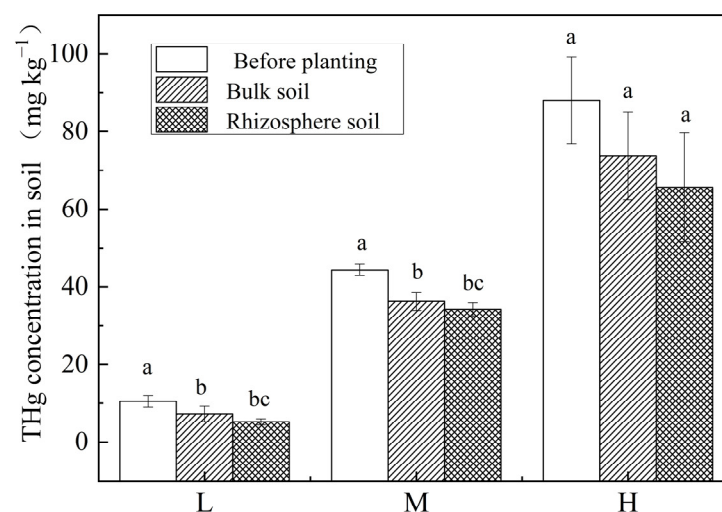


**Figure 1.** Soil THg concentrations in the plots with different levels of Hg contamination (different letters assigned for every treatment and bars with different letters are significantly different at  $p < 0.05$ ). Bulk soil and rhizosphere soil were analyzed after ramie planting.

The THg concentration was lower in rhizosphere soil than in the bulk soil. In plots L, M, and H, the rhizosphere soil THg concentration was 50.18%, 23.01%, and 25.43% lower than the bulk soil concentration after ramie planting, respectively. As shown in Table S1, pH and Eh were lower in rhizosphere soil than in bulk soil, whereas SOM and CEC were higher in rhizosphere soil than in bulk soil. CEC in rhizosphere soil significantly increased in the L and H plots, while rhizosphere soil Eh in the M plot obviously increased. The results indicated that soil properties in rhizosphere soil were different from bulk soil properties. Plants secrete a variety of root exudates into rhizosphere soil during their growth. Differences in root exudates, including sugars and amino acids, can influence soil properties, such as pH, SOM, Eh, and CEC [28]. Reducing soil pH could significantly increase HM bioavailability and even change HM speciation [29]. Low-molecular-weight organic acids produced by roots can solubilize HMs in the soil by forming complexes with HM ions, thereby allowing HM absorption by plants [24]. Soil Eh is a key factor affecting the speciation of HMs, which affects Hg methylation and demethylation [1]. In addition, increasing CEC facilitates the absorption of HM ions by plant roots. The differences in pH, Eh, SOM, and CEC between rhizosphere and bulk soil indicate that rhizosphere factors can alter Hg bioavailability and improve Hg phytoremediation efficiency in the root region. Soil properties also function as environmental variables that regulate the soil microbial community and thus influence the roles of microbes in changes in Hg speciation [29]. Redundancy analysis (RDA) in Figure 2 show that, in our study, CEC and Eh were the main factors influencing THg. This may be due to the special soil properties.

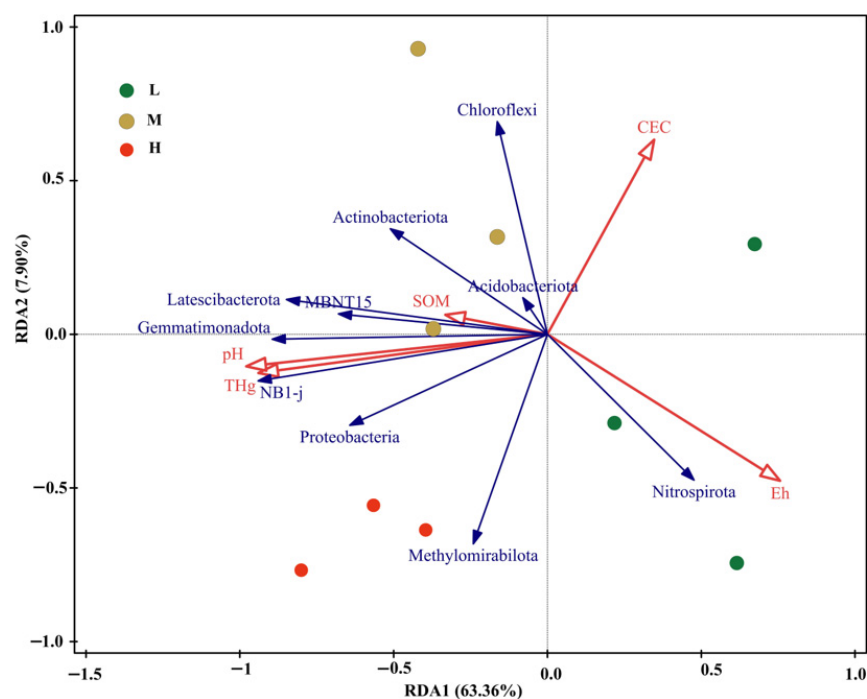


**Figure 2.** Redundancy analysis (RDA) of the correlations between soil environmental variables and bacterial community structure at the phylum level.

To characterize the distribution of Hg in different ramie tissues, the concentrations of Hg in ramie roots, stems, bast, and leaves were determined (Figure 3). The concentrations of Hg in plot L were 36.29, 129.83, 216.04, and 490.60  $\mu\text{g}\cdot\text{kg}^{-1}$  in the stems, bast, roots and leaves, respectively; in plot M, 56.56, 225.23, 308.01, and 634.28  $\mu\text{g}\cdot\text{kg}^{-1}$ , respectively; and in plot H, 84.31, 324.28, 502.78, and 1424.10  $\mu\text{g}\cdot\text{kg}^{-1}$ , respectively. In all plots, the concentration of THg in plant tissues followed the following order: leaves > bast > roots > stems. These results showed that Hg is absorbed by ramie roots and translocated to the aerial parts. However, the leaf content of Hg was significantly higher than the contents

of Hg in the roots, stems, and bast ( $p < 0.05$ ). Zhu et al. reported that Hg differs from most HMs (such as Cd) because it is primarily absorbed by plant leaves [8]. Plants absorb Hg from the soil, transform it, and release it to the atmosphere in gaseous form through their aboveground parts [2]. This transformation mechanism was reported in *Brassica juncea* [30]. It is also a protective strategy for ramie to be tolerant to Hg contamination. At the same time, ramie planting could stimulate soil microorganisms in the rhizosphere by secreting various root exudates. Soil microorganisms can easily transform  $\text{Hg}^{2+}$  into  $\text{Hg}^0$ , which can be volatilized and absorbed by plant leaves [31]. Furthermore, the rough, large leaves of ramie facilitate Hg accumulation. Perhaps these were the reasons behind ramie showing significant accumulation capability in its leaves.

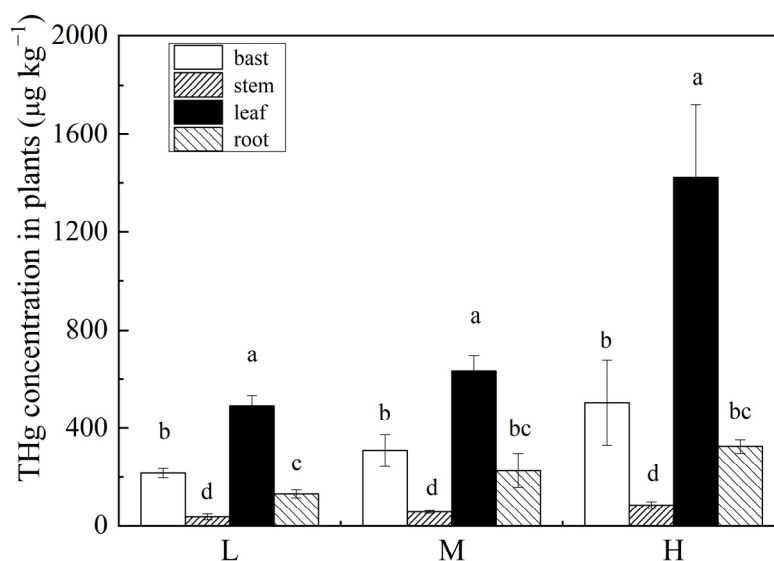


**Figure 3.** THg contents in ramie roots, leaves, stems, and bast in the plots with different levels of Hg contamination (different letters assigned for every treatment and bars with different letters are significantly different at  $p < 0.05$ ).

### 3.2. Changes of Hg Chemical Fractions between Bulk Soil and Rhizosphere Soil

The chemical fractions of Hg in bulk soil and rhizosphere soil are shown in Figure 4. The proportion of different chemical fractions of soil Hg were similar in the three plots both in bulk soil (Figure 4A) and in rhizosphere soil (Figure 4B). Residual fraction Hg (F5) and organic matter-binding fraction Hg (F4) were the major fractions. Exchangeable-fraction Hg (F1), carbonate-binding fraction Hg (F2), and Fe–Mn-oxide-binding fraction Hg (F3) collectively accounted for less than 10% of THg. Similar results were reported by Yin et al. [32] who found that 64–81% of Hg in Tongren soils was associated with metacinnabar ( $\beta$ -HgS). Compared to bulk soil (Figure 4A), organic-matter-binding fraction Hg (F4) was lower in rhizosphere soil (Figure 4B), whereas exchangeable-fraction Hg (F1), carbonate-binding fraction Hg (F2), and Fe–Mn-oxide-binding fraction Hg (F3) were higher in rhizosphere soil (Figure 4B). These results demonstrate that the chemical fractions of Hg are transformed in rhizosphere soil. Plant roots release many root exudates that sustain a rich microbial community in the rhizosphere. Those acidic root exudates could promote the transformation of Hg from species with low mobility and bioavailability to those with high bioavailability [24]. In addition, Hg contamination in the soil stimulates Hg-resistant bacteria, some of which were useful for the transformation of chemical fractions of Hg [28].

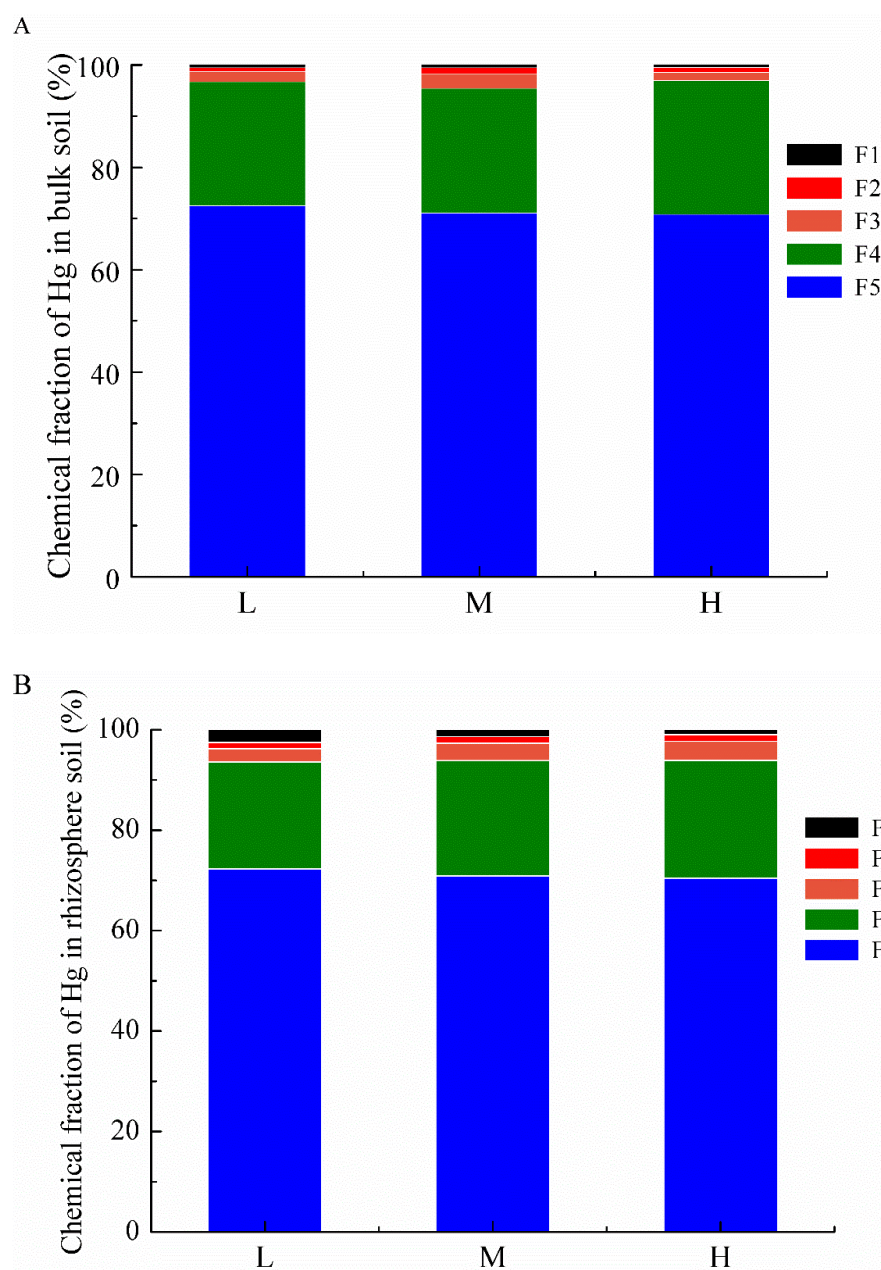


**Figure 4.** Percentages of different chemical forms of Hg in bulk (A) and rhizosphere (B) soil.

### 3.3. Diversity and Structure of the Soil Bacterial Community in Hg-Contaminated Soils

#### 3.3.1. Bacterial $\alpha$ -Diversity

A total of 2,755,752 bacterial sequences were retrieved after filtering low-quality reads. In total, 9363 bacterial OTUs were recovered from these sequences. As shown in Figure S1, the total number of OTUs was highest in plot L (5584 OTUs) and lowest in plot H (5249 OTUs). In addition, the number of unique OTUs was highest in plot L and lowest in plot H. These results suggest that a high soil Hg concentration restricts the number of bacteria. A similar result was reported by Wu et al. [11].

As shown in Table S2, the species richness (observed species, Chao, and ACE) and diversity (Shannon and Simpson) did not differ significantly among the three plots ( $p > 0.05$ ). The stability of the microbial community structure can be reflected by the community diversity. Diversity is a comprehensive indicator of community richness and evenness. The observed species, Chao, and ACE indices are commonly used to evaluate community richness, and the Shannon and Simpson indices are used to measure community diver-

sity [33]. Soil contamination by Hg is expected to alter microbial community structure. However, there were no remarkable differences in all plots. Mining and smelting activities in Tongren district ended in the 1980s; thus, the soil has been exposed to Hg contamination for more than 40 years [34], a sufficient period for adaptation. Consequently, the lack of significant differences in bacterial diversity among the plots is not surprising. Nonetheless, the observed species, Chao, and ACE indices were all highest in plot M (Table S2). This trend suggests that under Hg stress, the number of Hg-resistant bacteria in the soil initially increased but then decreased as the Hg concentration and associated stress increased further. As a result, the  $\alpha$ -diversity of the soil bacterial community was highest in moderately Hg-polluted soil. Liu et al. [16] also reported that bacterial diversity tended to increase under moderate Hg contamination.

### 3.3.2. Bacterial $\beta$ -Diversity

Bacterial  $\beta$ -diversity was analyzed with PCoA. As shown in Figure S2, the bacterial communities in the three plots were clearly separated, which indicates that their bacterial community structures were significantly different due to differences in Hg content. Bacterial  $\beta$ -diversity analysis was conducted to reveal evolutionary similarities and differences among the bacterial communities in the different Hg-contaminated soils. Principal coordinate analysis (PCoA) uses variance decomposition to visualize differences between multiple sets of data on a two-dimensional coordinate graph [14]. The two axes are the components that explain the variance with the maximum eigenvalues. Bacterial communities that are more similar in composition are located closer to one another on the PCoA map. The second principal component (PCoA2) discriminated the bacterial communities in plots M and H from those in plot L. Thus, as the soil concentration of Hg increased, the bacterial community structure changed. These changes may include increases in the abundance of potential Hg-resistant species to maintain soil ecological stability, which led to significant differences in soil microbial community structures between plots M and H and plot L. These results suggest that the bacterial communities in minimally Hg-contaminated soil was different from that in significantly Hg-contaminated soil, and the level of Hg contamination drove similarities and differences in the evolution of the soil bacterial community. Pu et al. also confirmed that Hg contamination significantly changes soil microbial community structures, and Hg level was the most important predictor of microbial profiles in their study [35].

### 3.3.3. Abundances of Bacterial Phyla

The soil bacterial community composition in the three plots is shown in Figure 5. Proteobacteria was the most abundant phylum in all plots, followed by Acidobacteriota, Actinobacteriota, and Chloroflexi. The four phyla were dominant in the soils and accounted for more than 78% of the bacterial sequences. NB1-j, Nitrospirota, Latescibacterota, MBNT15, Gemmatimonadota, Bacteroidota, Myxococcota, Crenarchaeota, and Verrucomicrobiota were present at low abundance in the three plots. Compared to plot L, the relative abundances of Proteobacteria, Actinobacteriota, Gemmatimonadota, Latescibacterota and NB1-j were higher in plots M and H, whereas the relative abundances of Acidobacteriota, Chloroflexi, and Nitrospirota were lower. Previous studies of HM-contaminated soil have reported that Proteobacteria are the dominant flora and resistant microorganisms. Proteobacteria can biomineralize HMs, and an increase in the abundance of Proteobacteria could indicate resistance of soil microorganisms to toxic substances [14]. Another abundant phylum, Actinobacteriota, is capable of degrading soil organic matter and toxic inorganic compounds in soil [36]. Under high Hg stress, these metal-resistant bacteria are stimulated, and an abundance of these bacteria increase. Gemmatimonadota, Latescibacterota, and NB1-j are all Hg tolerant. When stimulated by long-term Hg stress, these phyla promote increases in the relative abundance of resistant species to maintain their ecological stability [31]. Acidobacteriota, Chloroflexi, and Nitrospirota are sensitive to Hg stress, and obvious decreases in their abundance have been observed in soils with high Hg contami-

nation [31]. Our results indicate that the level of Hg contamination influenced taxonomic composition; these shifts in the bacterial community may be the result of ecological selection to adapt to the environment.

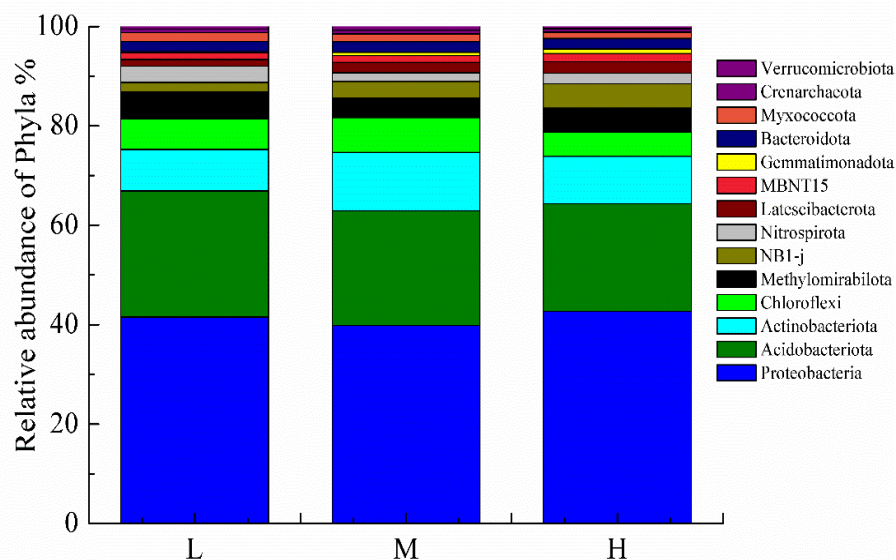


**Figure 5.** The relative abundances of the predominant bacterial taxa at the phylum level.

### 3.4. Differentially Abundant Biomarkers in Plots with Different Levels of Hg Contamination

LEfSe analysis was performed to identify the predominant discriminant taxa at the phylum and class levels in the soil bacterial communities in the three plots. As shown in Figure 6, 12, 4, and 14, differentially abundant clades were identified in plots L, M, and H, respectively. In plot L, Alphaproteobacteria in the phylum Proteobacteria, Acidobacteriae in the phylum Acidobacteriota, Gemmatimonadaceae in the phylum Gemmatimonadetes, Nitrospira in the phylum Nitrospirota, and Candidatus in the phylum Verrucomicrobiota were more abundant. In plot M, Thermoleophilia in the phylum Actinobacteriota and Acidimicrobiia in the phylum Actinobacteriota were highly abundant. The major bacterial classes identified in plot H were Burkholderiales, Steroidobacterales, and Azospirillales in the phylum Proteobacteria; Vicinamibacteria; and NB1-j. Previous studies have demonstrated that the Hg resistance gene (*merA*) is mainly distributed in Proteobacteria, Actinobacteriota, and Gemmatimonadetes [31]. Members of Proteobacteria are associated with the iron and sulfur cycles in soil and include various metallophilic bacteria. Betaproteobacteria include taxa that have been found in highly HM-contaminated soil. These bacteria can tolerate high metal content and even biomineralize metallic elements [14]. In particular, Burkholderiales, a member of Betaproteobacteria, is an order of Hg-tolerant and important plant-growth promoting bacteria that can enhance HM phytoremediation [13]. Burkholderiales was the predominant discriminant taxon in plot H and thus could be used as a biomarker of highly Hg-polluted soil.

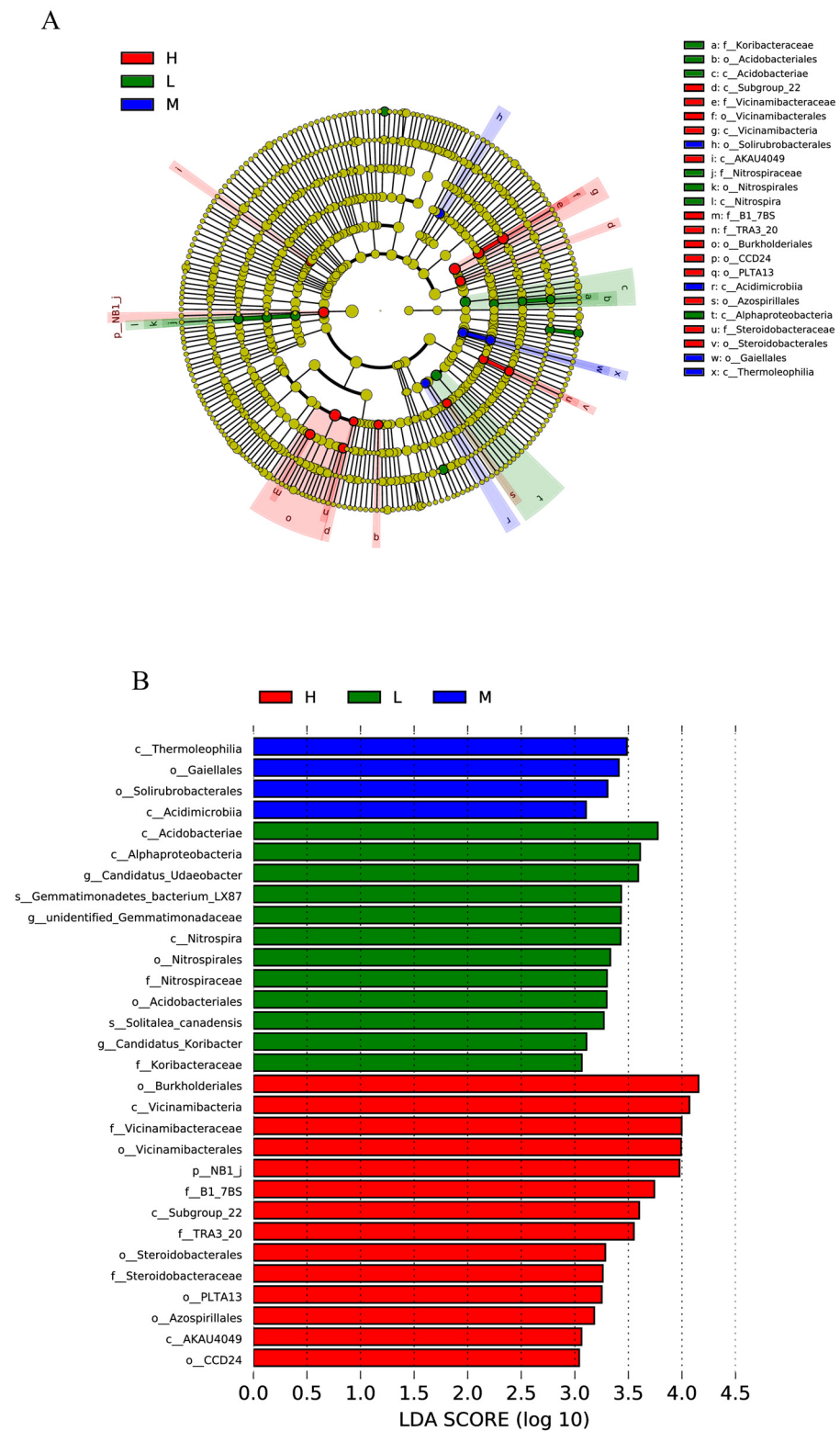


**Figure 6.** LEfSe analysis of soil bacteria in the three plots. Figure (A) shows the phylogenetic dendrogram of biomarker bacteria, and Figure (B) shows the most differentially abundant biomarkers and their LDA scores.

### 3.5. Effects of Environmental Variables on the Bacterial Community

As shown in Figure 2, soil pH, Eh, and THg were the strongest drivers of changes in the bacterial community. Some Hg-resistant bacteria, such as Proteobacteria, NB1-j, Methy-

lomirabilota, and Gemmatimonadota, were more predominant in plot H than in plots L and M. The relationships between soil environmental factors and the ten most abundant phyla were further assessed using Spearman correlation analysis (Figure S3). THg was positively correlated with NB1-j and negatively correlated with Verrucomicrobiota; pH was positively correlated with NB1-j and negatively correlated with Verrucomicrobiota and Bacteroidota; and Eh was positively correlated with Bacteroidota and negatively correlated with Actinobacteriota. Phytoremediation efficiency was related to changes in the rhizosphere environment, such as soil physicochemical properties and microbial community structure. These relationships indicate that plant root exudates in the rhizosphere can alter soil pH, SOM, Eh, and CEC, resulting in changes in soil microbial community structure. At the same time, the rhizosphere soil microorganisms can use these root exudates to improve HM bioavailability and thus increase phytoremediation efficiency. Our results suggested that the phytoremediation was performed by both plants and their rhizospheric bacteria. The interactions between plant and microbe were sustainable for remediation of Hg-contaminated soil [37].

#### 4. Conclusions

In summary, this study investigated the phytoremediation potential and rhizosphere bacterial characteristics of ramie in three plots with different levels of Hg contamination. The results showed that ramie is a promising candidate for Hg phytoremediation. Leaves were the major plant part responsible for Hg accumulation. After phytoremediation, Hg chemical fractions in rhizosphere soil changed. The proportion of exchangeable fraction Hg, carbonate-binding fraction Hg and Fe–Mn-oxide-binding fraction Hg increased. In addition, the abundance and composition of the rhizosphere bacterial community varied among the plots with different levels of Hg contamination. Those Hg-resistant bacteria phyla such as Proteobacteria, Actinobacteriota, Gemmati-monadota, Latescibacterota, and NB1-j increased in the plots with high levels of Hg. Burkholderiales was the predominant discriminant taxon in highly Hg-contaminated soil. Soil properties in rhizosphere soil were different from bulk soil. Among them, soil pH, Eh, and THg were the main factors driving the soil bacterial community. The phytoremediation of Hg contaminated soil by ramie involves the combined work of plants and their rhizospheric bacteria. This work provides a foundation for predicting the phytoremediation potential of ramie and the response of the rhizosphere microbial community as well as its potential functions regarding Hg contamination.

**Supplementary Materials:** The following supporting information can be downloaded at <https://www.mdpi.com/article/10.3390/su15076009/s1>. Figure S1: Unique bacterial OTUs in the three plots; Figure S2: PCoA of the soil bacterial community; Figure S3: Spearman correlation analysis of the soil environmental variables and the 10 most abundant phyla; Table S1: Soil properties in bulk soil and rhizosphere soil; and Table S2: Changes in the  $\alpha$ -diversity of the soil bacterial community.

**Author Contributions:** Writing—original draft preparation, formal analysis, and methodology, X.L.; conceptualization, writing—review and editing, X.W., Y.T., L.Z. and Y.L.; sample collection, sample determination and project administration, L.Z., Z.W.; funding acquisition, Y.T. All authors have read and agreed to the published version of the manuscript.

**Funding:** This research was funded by the National Key Research and Development Program of China (2019YFC1803705), and the Major Projects of the National Natural Science Foundation of China (41991335; 42130718).

**Institutional Review Board Statement:** Not applicable.

**Informed Consent Statement:** Not applicable.

**Data Availability Statement:** The data presented in this study are available on request from the corresponding author.

**Conflicts of Interest:** The authors declare no conflict of interest.

## References

1. Wang, J.; Shaheen, S.M.; Jing, M.; Anderson, C.W.N.; Swertz, A.-C.; Wang, S.-L.; Feng, X.; Rinklebe, J. Mobilization, Methylation, and Demethylation of Mercury in a Paddy Soil Under Systematic Redox Changes. *Environ. Sci. Technol.* **2021**, *55*, 10133–10141. [[CrossRef](#)]
2. Singh, A.D.; Khanna, K.; Kour, J.; Dhiman, S.; Bhardwaj, T.; Devi, K.; Sharma, N.; Kumar, P.; Kapoor, N.; Sharma, P.; et al. Critical review on biogeochemical dynamics of mercury (Hg) and its abatement strategies. *Chemosphere* **2023**, *319*, 137917. [[CrossRef](#)]
3. Zhang, H.; Feng, X.; Larssen, T.; Shang, L.; Vogt, R.D.; Rothenberg, S.E.; Li, P.; Zhang, H.; Lin, Y. Fractionation, distribution and transport of mercury in rivers and tributaries around Wanshan Hg mining district, Guizhou province, southwestern China: Part 1-Total mercury. *Appl. Geochem.* **2010**, *25*, 633–641. [[CrossRef](#)]
4. Saldarriaga, J.F.; Lopez, J.E.; Diaz-Garcia, L.; Montoya-Ruiz, C. Changes in *Lolium perenne* L. rhizosphere microbiome during phytoremediation of Cd- and Hg-contaminated soils. *Sci. Poll. Res. Int.* **2023**. [[CrossRef](#)]
5. Yang, B.; Zhou, M.; Shu, W.S.; Lan, C.Y.; Ye, Z.H.; Qiu, R.L.; Jie, Y.C.; Cui, G.X.; Wong, M.H. Constitutional tolerance to heavy metals of a fiber crop, ramie (*Boehmeria nivea*), and its potential usage. *Environ. Pollut.* **2010**, *158*, 551–558. [[CrossRef](#)]
6. Pandey, V.C.; Bajpai, O.; Singh, N. Energy crops in sustainable phytoremediation. *Renew. Sustain. Energy Rev.* **2016**, *54*, 58–73. [[CrossRef](#)]
7. Zhu, Q.H.; Huang, D.Y.; Liu, S.L.; Luo, Z.C.; Rao, Z.X.; Cao, X.L.; Ren, X.F. Accumulation and subcellular distribution of cadmium in ramie (*Boehmeria nivea* L. Gaud.) planted on elevated soil cadmium contents. *Plant Soil Environ.* **2013**, *59*, 57–61. [[CrossRef](#)]
8. Zhu, S.J.; Shi, W.J.; Zhang, J. Effect of different ramie (*Boehmeria nivea* L. Gaud) cultivars on the adsorption of heavy metal ions cadmium and lead in the remediation of contaminated farmland soils. *Open Chem.* **2022**, *20*, 444–454. [[CrossRef](#)]
9. Gong, X.M.; Huang, D.L.; Liu, Y.G.; Zeng, G.M.; Wang, R.Z.; Wan, J.; Zhang, C.; Cheng, M.; Qin, X.; Xue, W.J. Stabilized Nanoscale Zerovalent Iron Mediated Cadmium Accumulation and Oxidative Damage of *Boehmeria nivea* (L.) Gaudich Cultivated in Cadmium Contaminated Sediments. *Environ. Sci. Technol.* **2017**, *51*, 11308–11316. [[CrossRef](#)]
10. Xu, J.; Xing, Y.; Wang, J.; Yang, Y.; Ye, C.; Sun, R. Effect of poly-gamma-glutamic acid on the phytoremediation of ramie (*Boehmeria nivea* L.) in the Hg-contaminated soil. *Chemosphere* **2023**, *312*, 137280. [[CrossRef](#)]
11. Wu, B.H.; Luo, S.H.; Luo, H.Y.; Huang, H.Y.; Xu, F.; Feng, S.; Xu, H. Improved phytoremediation of heavy metal contaminated soils by *Miscanthus floridulus* under a varied rhizosphere ecological characteristic. *Sci. Total Environ.* **2022**, *808*, 151995. [[CrossRef](#)] [[PubMed](#)]
12. Hu, H.L.; Li, Z.H.; Xi, B.D.; Xu, Q.G.; Tan, W.B. Responses of bacterial taxonomic attributes to mercury species in rhizosphere paddy soil under natural sulphur-rich biochar amendment. *Ecotoxicol. Environ. Saf.* **2022**, *229*, 151995. [[CrossRef](#)] [[PubMed](#)]
13. Frossard, A.; Hartmann, M.; Frey, B. Tolerance of the forest soil microbiome to increasing mercury concentrations. *Soil Biol. Biochem.* **2017**, *105*, 162–176. [[CrossRef](#)]
14. Zhao, S.W.; Qin, L.Y.; Wang, L.F.; Sun, X.Y.; Yu, L.; Wang, M.; Chen, S.B. Soil bacterial community responses to cadmium and lead stabilization during ecological restoration of an abandoned mine. *Soil Use Manag.* **2022**, *38*, 1459–1469. [[CrossRef](#)]
15. Bach, E.M.; Williams, R.J.; Hargreaves, S.K.; Yang, F.; Hofmockel, K.S. Greatest soil microbial diversity found in micro-habitats. *Soil Biol. Biochem.* **2018**, *118*, 217–226. [[CrossRef](#)]
16. Liu, Y.R.; Delgado-Baquerizo, M.; Bi, L.; Zhu, J.; He, J.Z. Consistent responses of soil microbial taxonomic and functional attributes to mercury pollution across China. *Microbiome* **2018**, *6*, 183. [[CrossRef](#)]
17. Pignataro, A.; Moscatelli, M.C.; Mocali, S.; Grego, S.; Benedetti, A. Assessment of soil microbial functional diversity in a coppiced forest system. *Appl. Soil Ecol.* **2012**, *62*, 115–123. [[CrossRef](#)]
18. Luo, J.P.; Tao, Q.; Jupa, R.; Liu, Y.K.; Wu, K.R.; Song, Y.C.; Li, J.X.; Huang, Y.; Zou, L.Y.; Liang, Y.C.; et al. Role of Vertical Transmission of Shoot Endophytes in Root-Associated Microbiome Assembly and Heavy Metal Hyperaccumulation in Sedum alfredii. *Environ. Sci. Technol.* **2019**, *53*, 6954–6963. [[CrossRef](#)]
19. Frossard, A.; Donhauser, J.; Mestrot, A.; Gygax, S.; Baath, E.; Frey, B. Long- and short-term effects of mercury pollution on the soil microbiome. *Soil Biol. Biochem.* **2018**, *120*, 191–199. [[CrossRef](#)]
20. Hou, J.Y.; Liu, W.X.; Wu, L.H.; Ge, Y.Y.; Hu, P.J.; Li, Z.; Christie, P. *Rhodococcus* sp. NSX2 modulates the phytoremediation efficiency of a trace metal-contaminated soil by reshaping the rhizosphere microbiome. *Appl. Soil Ecol.* **2019**, *133*, 62–69. [[CrossRef](#)]
21. Li, X.H.; Zhao, L.; Teng, Y.; Luo, Y.M.; Huang, B.; Liu, B.L.; Zhao, Q.G. Characteristics, spatial distribution and risk assessment of combined mercury and cadmium pollution in farmland soils surrounding mercury mining areas in Guizhou. *Ecol. Environ. Sci.* **2022**, *31*, 1629–1636. (In Chinese)
22. Ata-Ul-Karim, S.T.; Cang, L.; Wang, Y.J.; Zhou, D.M. Interactions between nitrogen application and soil properties and their impacts on the transfer of cadmium from soil to wheat (*Triticum aestivum* L.) grain. *Geoderma* **2020**, *357*, 113923. [[CrossRef](#)]
23. Zhu, H.; Teng, Y.; Wang, X.; Zhao, L.; Ren, W.; Luo, Y.; Christie, P. Changes in clover rhizosphere microbial community and diazotrophs in mercury-contaminated soils. *Sci. Total Environ.* **2021**, *767*, 145473. [[CrossRef](#)] [[PubMed](#)]
24. Xu, S.; Gong, P.; Ding, W.; Wu, S.C.; Yu, X.W.; Liang, P. Mercury uptake by *Paspalum distichum* L. in relation to the mercury distribution pattern in rhizosphere soil. *Environ. Sci. Poll. Res.* **2021**, *28*, 66990–66997. [[CrossRef](#)]
25. Hou, J.Y.; Liu, W.X.; Wang, B.B.; Wang, Q.L.; Luo, Y.M.; Franks, A.E. PGPR enhanced phytoremediation of petroleum contaminated soil and rhizosphere microbial community response. *Chemosphere* **2015**, *138*, 592–598. [[CrossRef](#)]
26. Bussan, D.D.; Douvris, C.; Cizdziel, J.V. Mercury methylation potentials in sediments of an ancient cypress wetland using species-specific isotope dilution GC-ICP-MS. *Molecules* **2022**, *27*, 4911. [[CrossRef](#)]

27. Qiao, D.M.; Lu, H.F.; Zhang, X.X. Change in phytoextraction of Cd by rapeseed (*Brassica napus* L.) with application rate of organic acids and the impact of Cd migration from bulk soil to the rhizosphere. *Environ. Pollut.* **2020**, *267*, 115452. [[CrossRef](#)]
28. Sas-Nowosielska, A.; Galimska-Stypa, R.; Kucharski, R.; Zielonka, U.; Malkowski, E.; Gray, L. Remediation aspect of microbial changes of plant rhizosphere in mercury contaminated soil. *Environ. Monit. Assess.* **2008**, *137*, 101–109. [[CrossRef](#)]
29. Hao, X.D.; Bai, L.Y.; Liu, X.D.; Zhu, P.; Liu, H.W.; Xiao, Y.H.; Geng, J.B.; Liu, Q.J.; Huang, L.H.; Jiang, H.D. Cadmium Speciation Distribution Responses to Soil Properties and Soil Microbes of Plow Layer and Plow Pan Soils in Cadmium-Contaminated Paddy Fields. *Front. Microbiol.* **2021**, *12*, 774301. [[CrossRef](#)]
30. Moreno, F.N.; Anderson, C.W.N.; Stewart, R.B.; Robinson, B.H. Phytoremediation of mercury-contaminated water: Volatilisation and plant-accumulation aspects. *Environ. Exp. Bot.* **2008**, *62*, 78–85. [[CrossRef](#)]
31. Liu, Y.R.; Wang, J.J.; Zheng, Y.M.; Zhang, L.M.; He, J.Z. Patterns of Bacterial Diversity Along a Long-Term Mercury-Contaminated Gradient in the Paddy Soils. *Microb. Ecol.* **2014**, *68*, 575–583. [[CrossRef](#)] [[PubMed](#)]
32. Yin, R.S.; Gu, C.H.; Feng, X.B.; Hurley, J.P.; Krabbenhoft, D.P.; Lepak, R.F.; Zhu, W.; Zheng, L.R.; Hu, T.D. Distribution and geochemical speciation of soil mercury in Wanshan Hg mine: Effects of cultivation. *Geoderma* **2016**, *272*, 32–38. [[CrossRef](#)]
33. Wang, L.; Wang, L.A.; Zhan, X.Y.; Huang, Y.K.; Wang, J.; Wang, X. Response mechanism of microbial community to the environmental stress caused by the different mercury concentration in soils. *Ecotoxicol. Environ. Saf.* **2020**, *188*, 109906. [[CrossRef](#)]
34. Li, P.; Feng, X.; Shang, L.; Qiu, G.; Meng, B.; Liang, P.; Zhang, H. Mercury pollution from artisanal mercury mining in Tongren, Guizhou, China. *Appl. Geochem.* **2008**, *23*, 2055–2064.
35. Pu, Q.; Zhang, K.; Poulain, A.J.; Liu, J.; Zhang, R.; Abdelhafiz, M.A.; Meng, B.; Feng, X.B. Mercury drives microbial community assembly and ecosystem multifunctionality across a Hg contamination gradient in rice paddies. *J. Hazard. Mater.* **2022**, *435*, 129055. [[CrossRef](#)] [[PubMed](#)]
36. Alvarez, A.; Benimeli, C.S.; Saez, J.M.; Fuentes, M.S.; Cuzzo, S.A.; Polti, M.A.; Amoroso, M.J. Bacterial Bio-Resources for Remediation of Hexachlorocyclohexane. *Int. J. Mol. Sci.* **2012**, *13*, 15086–15106. [[CrossRef](#)]
37. Rane, N.R.; Tapase, S.; Kanojia, A.; Watharkar, A.; Salama, E.-S.; Jang, M.; Yadav, K.K.; Amin, M.A.; Cabral-Pinto, M.M.S.; Jadhav, J.P.; et al. Molecular insights into plant-microbe interactions for sustainable remediation of contaminated environment. *Bioresour. Technol.* **2022**, *344*, 126246. [[CrossRef](#)]

**Disclaimer/Publisher’s Note:** The statements, opinions and data contained in all publications are solely those of the individual author(s) and contributor(s) and not of MDPI and/or the editor(s). MDPI and/or the editor(s) disclaim responsibility for any injury to people or property resulting from any ideas, methods, instructions or products referred to in the content.